The Effects of Surface Evaporation Parameterizations on Climate Sensitivity to Solar Constant Variations

SHU-HSIEN CHOU AND ROBERT J. CURRAN

Laboratory for Atmospheric Sciences, Goddard Space Flight Center, Greenbelt, MD 20771

GEORGE OHRING

Department of Geophysics and Planetary Sciences, Tel-Aviv University, Ramat-Aviv, Israel

(Manuscript received 1 November 1979, in final form 18 November 1980)

ABSTRACT

The effects of two different evaporation parameterizations on the sensitivity of simulated climate to solar constant variations are investigated by using a zonally averaged climate model. One parameterization is a nonlinear formulation in which the evaporation is nonlinearly proportional to the sensible heat flux, with the Bowen ratio determined by the predicted vertical temperature and humidity gradients near the earth's surface (model A). The other is the formulation of Saltzman (1968) with the evaporation linearly proportional to the sensible heat flux (model B). The computed climates of models A and B are in good agreement except for the energy partition between sensible and latent heat at the earth's surface. The difference in evaporation parameterizations causes a difference in the response of temperature lapse rate to solar constant variations and a difference in the sensitivity of longwave radiation to surface temperature which leads to a smaller sensitivity of surface temperature to solar constant variations in model A than in model B. The results of model A are qualitatively in agreement with those of the general circulation model calculations of Wetherald and Manabe (1975).

1. Introduction

The transfer of latent heat from the earth's surface to the atmosphere is an important physical process. It is directly related to the determination of the surface temperature through the surface energy balance equation. It affects indirectly the latent heat release, cloud cover, temperature lapse rate and the dynamics of the atmosphere. Charney *et al.* (1977) adopted two different evaporation parameterizations in the Goddard Institute for Space Studies (GISS) general circulation model (GCM), and found that the difference in evaporation markedly affected cloud cover, precipitation, surface temperature, dynamical instabilities and related eddy activities. The GCM experiments of Wetherald and Manabe (1975, hereafter referred to as WM) found that the extra energy absorbed by the earth's surface due to the increase in the solar constant is primarily balanced by the removal of heat through evaporation. The response of the surface temperature to a climatic perturbation (e.g., changes in solar constant, CO_2 content) can therefore be expected to depend strongly on the efficiency of evaporation in transferring energy. Since evaporation is so important, its role in climate sensitivity studies needs to be explored.

Saltzman (1967) suggested a simple semi-empirical representation of the surface heat balance equation for computing the earth's surface temperature. In that study, the latent heat flux (evaporation) was assumed to be linearly proportional to the sensible heat flux at the earth's surface with the coefficients determined from the heat budgets at 45°N for January and July. This linear formulation of evaporation was further used in several statistical-dynamical climate models to simulate the observed climate (e.g., Saltzman, 1968; Saltzman and Vernekar, 1971, 1972; Ohring and Adler, 1978; Vernekar and Chang, 1978).

In the present study, we compare this linear parameterization of evaporation with a nonlinear one. The nonlinear parameterization utilizes a simple boundary layer from which the Bowen ratio can be determined from the predicted vertical gradients of temperature and water vapor near the earth's surface (see Section 2).

The comparison of evaporation parameterizations is made with the use of a zonally averaged climate model based on the annual mean model of Ohring and Adler (1978, hereafter referred to as OA) with some modifications to the heating parameterizations. The model with the nonlinear evaporation formulation is referred to as model A, and that with the linear one is referred to as model B. The climates

0022-4928/81/050931-08$06.00

predicted by these two models, as well as the sensitivity of model climates to changes in the solar constant, are studied.

2. Description of the climate models

Since the basic climate model has been described fully in OA, we present here only a short summary of its main characteristics. Further details may be found in OA. The two different evaporation formulations as well as some changes introduced into the OA model are described more fully.

a. Basic model

The dynamical model is the standard two-level quasi-geostrophic model, with the atmosphere divided into two layers, 0–500 mb and 500–1000 mb. The governing equations are the zonally averaged quasi-geostrophic potential vorticity equations, which can be obtained by combining the vorticity equation and the thermodynamic energy equation (Sela and Wiin-Nielsen, 1971; Wiin-Nielsen and Fuenzalida, 1975). The 500 mb temperatures are computed from a diagnostic equation for the thermal stream function, and the surface temperatures (at 1000 mb) are obtained from the surface energy balance equation. The surface heating $H_s(i)$ and the atmospheric heating $H_a(i)$ processes considered are solar radiation, longwave radiation, convection, evaporation, latent heat release, and oceanic transport. While the solar and longwave radiation calculations are fairly detailed, the other diabetic heating processes are highly parameterized.

b. Evaporation parameterizations

In both parameterizations, the energy used in evaporating water from the earth's surface $H_s(4)$, is related to the sensible heat flux from the earth's surface to the atmosphere, $H_s(3)$, which follows Saltzman's (1968) formulation

$$H_s(3) = -b(T_s - T_5) + c, \tag{1}$$

where T_s and T_5 are temperatures at 1000 mb and 500 mb, respectively, and b and c are constants independent of latitude.

In model A, we assume a relationship between latent and sensible heat fluxes with the coefficient of proportionality determined internally, thus making this a nonlinear formulation. In model B, we use the formulation of Saltzman (1968) which relates the latent heat flux linearly to the sensible heat flux with fixed coefficients independent of latitude. The parameterizations of evaporation for models A and B are then

$$H_s(4) = WeH_s(3) \quad \text{(model A)}, \tag{2}$$

$$H_s(4) = W[e'H_s(3) + f'] \quad \text{(model B)}, \tag{3}$$

where W is a water availability factor depending on the relative amount of ocean, land, sea ice and snow at each latitude belt, and is assumed to be 1 for ocean, 0.8 for land and 0 for ice and snow (Saltzman and Vernekar, 1971). The quantities e' and f' are constants, and e is determined from the vertical gradients of water vapor and temperature near the earth's surface

$$e = [L(q_s^* - q_B)]/[c_p(T_s - T_B)]. \tag{4}$$

Here q is the specific humidity, T the temperature, subscripts s and B refer to the 1000 mb level and the top of the boundary layer P_B, respectively; q_s^* is the saturated q at 1000 mb, L the latent heat of condensation, and c_p the specific heat at constant pressure. The quantity e is equivalent to the inverse of the Bowen ratio for a saturated surface. In the general circulation models, P_B is usually chosen to be the lowest prognostic level (e.g., Manabe, 1969). In this study, P_B is specified such that the Bowen ratio $(We)^{-1}$ of the standard case (simulation of the present climate) in each latitude belt is close to its climatological value. The coefficient e and the sensible heat flux are determined from the predicted temperature field. Therefore, (2) is a nonlinear relationship between sensible and latent heat fluxes. For the linear formulation of (3) which also was used by OA, the relative response of latent and sensible heat to a climatic perturbation is essentially determined by the prescribed constant e'. The ratio of the change in latent heat to the change in sensible heat due to any perturbation is equal to We', if ice/snow covers remain unchanged. This ratio is determined by the model when (2) is used.

The constants e', f' and b are identical to those suggested by Saltzman (1968), based upon his analysis of the heat budget at 45°N latitude. The constant c was modified from Saltzman's (1968) suggested value in the course of tuning experiments with the model (see Section 3).

c. Changes to OA

For an equilibrium condition, latent heat release in an atmospheric column is equal to the latent heat flux from the earth's surface plus the convergence of water vapor by atmospheric circulation. It was assumed in OA that the flux convergence of water vapor by atmospheric motion is proportional to the deviation of zonally averaged cloud amount from its hemispheric average. In the present model, we compute the flux convergence of water vapor from the computed surface temperature and the prescribed vertical profiles of meridional wind and water vapor, as suggested by Sellers (1973). Except that a value of the eddy diffusivity for water vapor of about three times that used by Sellers (1973) was used in order to better simulate the meridional

TABLE 1. Parameters for surface albedo calculation.

Parameter	Season	Latitude (°N)								
		5	15	25	35	45	55	65	75	85
Land reflectivity		0.08	0.13	0.18	0.16	0.15	0.16	0.16	0.16	0.16
Ocean reflectivity	DJF	0.06	0.06	0.08	0.10	0.13	0.17	0.19	0.23	0.23
	MAM	0.06	0.06	0.06	0.07	0.08	0.09	0.11	0.13	0.13
	JJA	0.06	0.06	0.06	0.06	0.07	0.08	0.09	0.10	0.10
	SON	0.06	0.06	0.07	0.08	0.10	0.12	0.14	0.15	0.15
Fraction of solar radiation	DJF	0.24	0.23	0.18	0.15	0.11	0.07	0.03	0	0
	MAM	0.27	0.28	0.28	0.29	0.31	0.36	0.38	0.38	0.37
	JJA	0.24	0.75	0.30	0.34	0.38	0.42	0.50	0.57	0.59
	SON	0.25	0.24	0.24	0.22	0.20	0.15	0.09	0.05	0.04
Ocean fraction	DJF	0.78	0.72	0.62	0.56	0.48	0.37	0.14	0.10	0
	MAM	0.78	0.72	0.62	0.56	0.48	0.37	0.14	0.09	0
	JJA	0.78	0.72	0.62	0.56	0.48	0.42	0.20	0.17	0.01
	SON	0.78	0.72	0.62	0.56	0.48	0.42	0.22	0.26	0.01
Land fraction	DJF	0.22	0.28	0.38	0.38	0.15	0.05	0.01	0	0
	MAM	0.22	0.28	0.38	0.44	0.37	0.24	0.10	0.01	0
	JJA	0.22	0.28	0.38	0.44	0.52	0.55	0.59	0.12	0.01
	SON	0.22	0.28	0.38	0.44	0.43	0.35	0.28	0.05	0.01
Sea ice fraction	DJF	0	0	0	0	0	0.06	0.16	0.61	0.94
	MAM	0	0	0	0	0	0.06	0.16	0.62	0.94
	JJA	0	0	0	0	0	0.01	0.10	0.54	0.93
	SON	0	0	0	0	0	0.01	0.08	0.45	0.92
Snow fraction	DJF	0	0	0	0.06	0.37	0.52	0.69	0.29	0.06
	MAM	0	0	0	0	0.15	0.33	0.60	0.28	0.06
	JJA	0	0	0	0	0	0.02	0.11	0.17	0.05
	SON	0	0	0	0	0.09	0.22	0.42	0.24	0.06

transport of water vapor. Sellers (1973) implies that his assumed value of eddy diffusivity for water vapor may have been too small.

There are a number of minor differences between the present model and OA in the treatment of the surface albedo and the effective cloud layer. Rather than dwell on these differences, which are not relevant to the present investigation, we simply summarize the present formulations.

The earth's surface is assumed to consist of four surface types, i.e., open ocean, snow free land, snow and sea ice. The annual mean surface albedo at each latitude is computed as

$$r(\phi) = \sum_{j=1}^{4} \sum_{i=1}^{4} f_j(\phi) n_{ij}(\phi) r_{ij}(\phi),$$

where i is the index for the surface type, j the index for season, $r_{ij}(\phi)$ the reflectivity of surface type i at latitude ϕ during season j, $n_{ij}(\phi)$ the fraction of latitude belt covered by surface type i during season j, and $f_j(\phi)$ the weighting function accounting for the seasonal change in solar radiation. The seasonal values of $f(\phi)$, shown in Table 1, are computed from the data of Budyko (1963). Table 1 also shows the reflectivities of ocean and land, and the observed surface type coverages of Curran *et al.* (1978). Land reflectivities are taken from Sellers (1973) and vary only with latitude. Ocean reflectivities are taken from Budyko (1974) and vary with latitude and season. the reflectivities of snow and sea ice are made to depend on surface temperature. Following Weatherald and Manabe (1975), sea ice and snow are classified into stable and unstable types. Referring to the surface albedo study of Posey and Clapp (1964), the reflectivities of unstable sea ice and snow are assigned to be 0.4 and 0.5, respectively; those of stable sea ice and snow are 0.6 and 0.7, respectively.

Since the unstable snow/ice is usually associated with higher surface temperature and smaller snow/ice coverage as compared with stable types, the discrimination between the stable and unstable snow (or sea ice) is made according to the fraction of land covered by snow (or ocean covered by sea ice) in each latitude belt in each season. The critical fraction is taken to be 0.5.

In order to incorporate the feedback mechanism between snow/ice albedo and surface temperature, the snow/ice covers are computed from the model through some empirical relationships between the snow/ice cover and the surface temperature. Since only the annual mean surface temperatures (not the seasonal mean surface temperature) are computed

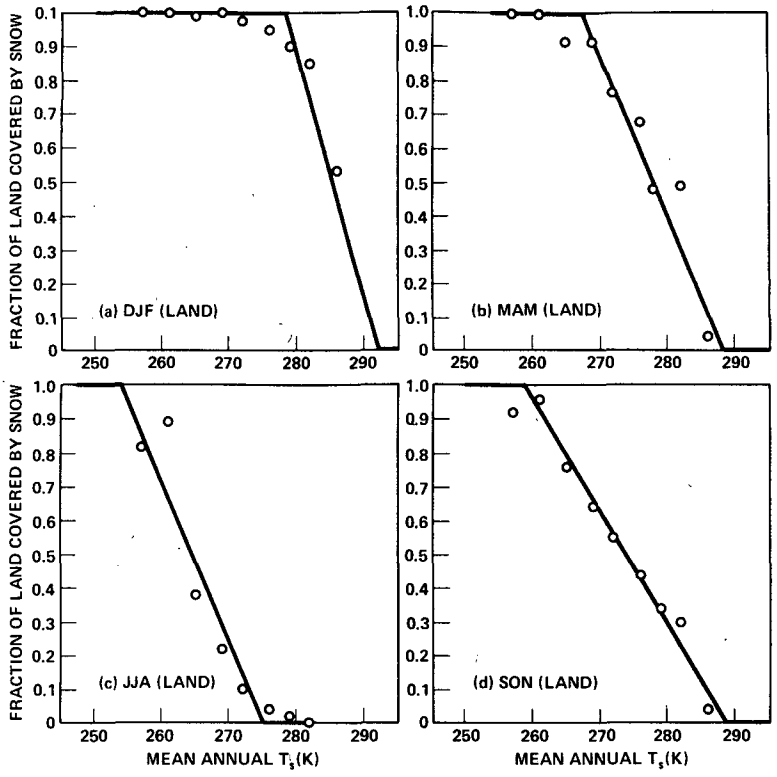

FIG. 1. Relationships between seasonal snow cover over land and the mean annual surface temperature.

from the model, the seasonal snow and sea ice covers are related to annual mean surface temperatures. The seasonal linear relationships for snow and sea ice and the data on which they are based are shown in Figs. 1 and 2. These are derived from the surface temperature data of Oort and Rasmusson (1971) and Newell *et al.* (1972), and the snow/ice cover of Curran *et al.* (1978). The sea ice cover data of Curran *et al.* are from the arctic sea ice analyses of the U.S. Navy Fleet Weather Facility for the period of 1972–75, and the snow cover data are inferred from the ESSA, ITOS, NOAA and SMS-1 satellites for the period of 1966–75. The empirical relationships of Figs. 1a, 1c, 2a and 2c for the winter and summer seasons were made available for Ohring and Adler (1978) to use in their model. For the experiments with ice-albedo feedback, the seasonal ice and snow covers are computed from the model through these linear relationships, but the observed snow and ice covers (Table 1) are used for the experiments without this feedback mechanism.

In order to compute the radiation fluxes, clouds are parameterized into a single cloud layer with the amounts the same as in OA. The effective cloud top and base are different from those of OA and are determined from the cloud statistics of London (1957). In computing the height of the effective cloud top, we first determine the amount of each cloud type not overlapped by upper cloud, assuming that cloud are randomly distributed. The height of the effective cloud top is then determined by weighting the six cloud-top heights of London by their respective non-overlapped cloud amounts. The height of the effective cloud base is computed in a similar way except that the non-overlapped cloud amounts are determined by viewing the sky from the ground. The effective cloud layer is assumed to be radiatively black to longwave radiation. Since the optical properties of Ci clouds are quite different from other cloud types, we have subjectively reduced the non-overlapping cloud amount of Ci by half in determining the effective cloud top and base. As shown in Table 2, the effective cloud top and base are ~1 km lower than those of OA, and the mean cloud top and base are ~4.7 and 2.7 km, respectively.

The optical thickness τ_c of the single cloud layer is determined from the six cloud types by considering overlapped clouds. Following Stone *et al.* (1977), the optical thickness of Ci, As, St, Ns, Cu and Cb are taken to be 2, 6, 8, 16, 16 and 32, respectively, for determining τ_c of the effective cloud layer. Since the absorption of solar radiation by cloud droplets and dust is not included, the single-scatter-

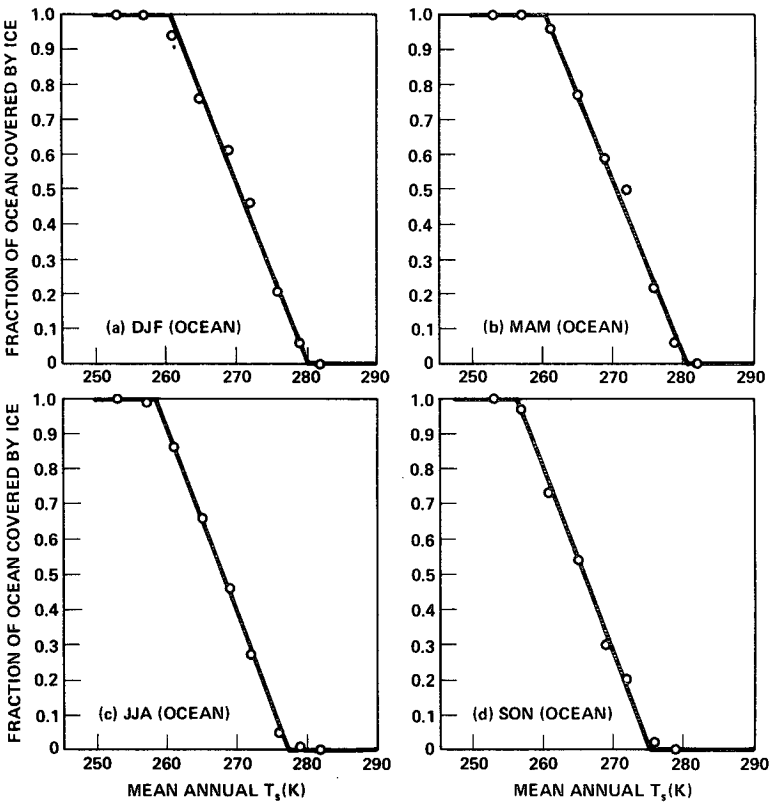

FIG. 2. Relationships between seasonal ice cover over ocean and the mean annual surface temperature.

ing albedo of the cloud is overestimated.[1] This together with the neglect of the absorption of solar radiation by O_2 and CO_2 further causes an overestimation in the planetary albedo. Therefore, the values of τ_c must be adjusted such that the planetary albedo and surface temperature compare well with the observations. A value of $\tau_c = 7$ was used by OA to simulate the observed climate and we have used this value as a reference for adjusting τ_c. The hemispheric mean value of τ_c derived from Stone *et al.* (1977) is about 11.5, which is 4.5 larger than that used by OA. In this study, the latitudinal distribution of τ_c derived from Stone *et al.* is reduced by an amount of 4.5 in each latitude belt. Values of τ_c used in this study are shown in Table 2. It is smaller in the subtropics and larger in the tropics and the middle latitudes. However, the latitudinal variation in τ_c is small.

[1] OA added 0.08 cm of water vapor to the cloud layer to account for the absorption by cloud droplets. According to our analysis, this only increases the surface temperature by <0.1°C. Since the liquid water content of the cloud is not well-known, we simply neglect this addition and retain the original Lacis and Hansen (1974) routine in this respect.

3. Results

a. *Simulation of observed climate*

The meridional variations and hemispheric mean values of surface and 500 mb temperatures for

TABLE 2. Latitude dependent parameters.*

Parameters	Latitude (°N)								
	0	10	20	30	40	50	60	70	80	90
Cloud-top height Z_t (km)	5.5	5.3	5.1	4.8	4.3	3.8	3.8	3.2	3.2	
Cloud-base height Z_b (km)	2.9	3.1	3.3	3.1	2.5	2.1	1.8	1.7	1.6	
Cloud optical thickness τ_c	7.6	7.1	6.6	6.5	6.8	7.1	7.2	7.0	6.6	
Boundary layer top P_B (mb)	930	930	930	940	970	985	996	999	999	

* Values of other latitude-dependent parameters are the same as those in OA.

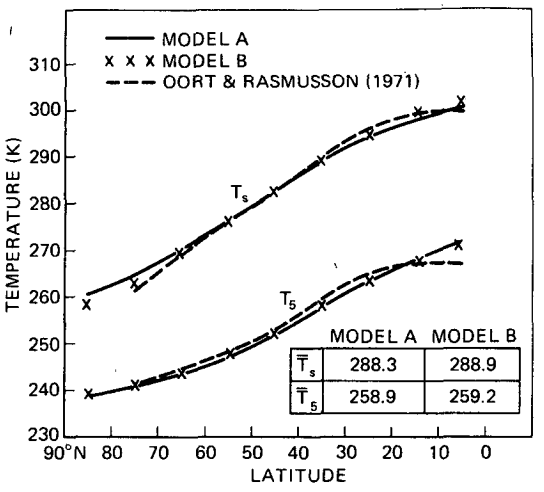

FIG. 3. Latitudinal distributions of surface (T_s) and 500 mb temperatures (T_5) for models A and B, together with the observed values from Oort and Rasmusson (1971). Overbar indicates hemispheric mean.

models A and B, together with the observed values (Oort and Rasmusson, 1971), are shown in Fig. 3. The computed temperatures of models A and B agree with one another and with the observed climatic values. However, to simulate correctly the observed temperatures, different values of c in (1) were necessary for the two models: for model A, a value of -190 cal cm^{-2} day^{-1} was required, while for model B, a value of -170 cal cm^{-2} day^{-1} was used.

The major difference in the climatic simulations of models A and B lies in the energy partition between sensible and latent heat fluxes at the earth's surface, as shown in Fig. 4. With the linear evaporation formulation (model B), the sensible heat flux is overestimated and the latent heat flux is underestimated, especially at low latitudes. Thus, although both models are equally successful in simulating the observed temperatures, model A with its nonlinear evaporation formulation simulates more correctly the observed sensible and latent heat fluxes.

b. Sensitivity to solar constant variations

The major purpose of this work is to examine the effects of the two different evaporation parameterizations on the sensitivity of the computed temperatures to variations in the solar constant. But, aside from different evaporation parameterizations, model A and B have different values of c in the sensible heat parameterization. Thus, the first step was to investigate the effect of these different values of c on the sensitivity of the model to solar constant variations. This was done by running model B with two values of c: -190 and -170 cal cm^{-2} day^{-1}. For a 1% change in the solar constant, the surface temperature changes were about the same for these two values of c. Therefore, any differences in the sensitivity of model A and B to solar constant variations can be attributed to different evaporation formulations.

Table 3 shows the temperature changes resulting from a 1% change in solar constant for models A and B. For the cases without ice-albedo feedback, the magnitude of the temperature change is essentially symmetric with respect to small changes in solar constant. Therefore, those changes corresponding to a 1% increase in solar constant are not shown in Table 3. As can be seen from Table 3, the sensitivity of surface temperature to solar constant variations is ~40% smaller in model A (nonlinear evaporation formulation) than in model B (linear evaporation formulation).

With the inclusion of the ice-albedo feedback mechanism, the maximum temperature change occurs at the surface level of the polar region for both models A and B. In low and middle latitudes, the temperature change is larger at the 500 mb level than at the earth's surface for model A, but the reverse is true for model B. The temperature lapse rate is therefore decreased in model A and increased in model B for an increase in solar constant. Using a GCM to perform the solar constant experiments, Wetherald and Manabe (1975) found that the

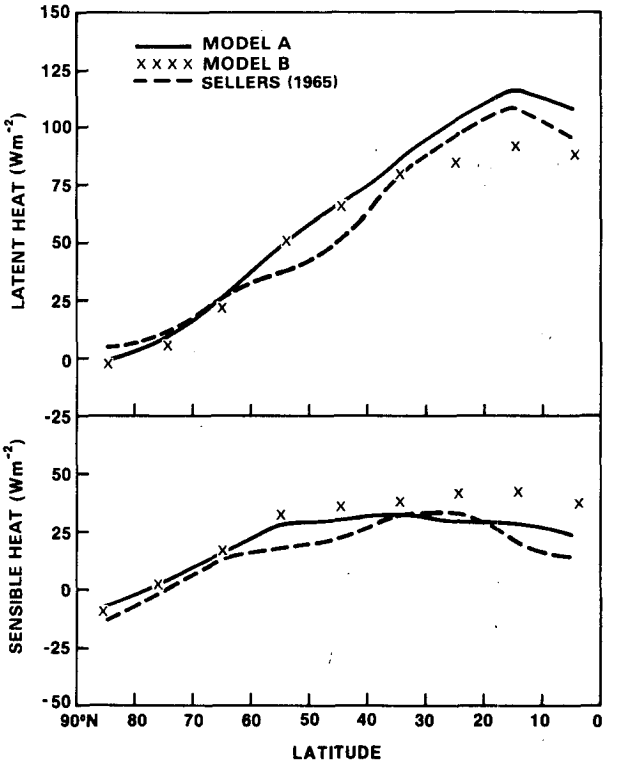

FIG. 4. Latitudinal distributions of the latent heat flux and the sensible heat flux at the earth's surface for models A and B, together with the observed values from Sellers (1965).

TABLE 3. Latitudinal distributions of temperature changes (k) at 500 and 1000 mb levels due to a 1% change in solar constant for models A and B.

P (mb)	Latitude (°N)	Model A			Model B		
		No ice feedback	Ice feedback		No ice feedback	Ice feedback	
		−1%	+1%	−1%	−1%	+1%	−1%
500	5	−0.9	0.9	−1.0	−1.0	1.2	−1.2
	15	−0.8	0.9	−0.9	−0.9	1.0	−1.0
	25	−0.8	0.9	−0.9	−0.8	1.0	−1.0
	35	−0.8	0.9	−1.0	−0.8	1.2	−1.2
	45	−0.8	1.1	−1.2	−0.9	1.5	−1.6
	55	−0.8	1.2	−1.3	−1.0	1.7	−1.8
	65	−0.8	1.3	−1.3	−1.0	1.8	−1.9
	75	−0.8	1.3	−1.4	−1.0	2.0	−2.0
	85	−0.8	1.4	−1.4	−1.0	2.1	−2.2
	Mean	−0.79	1.01	−1.05	−0.91	1.30	−1.36
1000	5	−0.7	0.8	−0.8	−1.1	1.2	−1.3
	15	−0.7	0.7	−0.7	−1.0	1.2	−1.2
	25	−0.6	0.7	−0.7	−1.0	1.2	−1.2
	35	−0.6	0.7	−0.7	−1.0	1.2	−1.3
	45	−0.6	0.8	−0.8	−1.0	1.3	−1.3
	55	−0.6	0.9	−0.9	−1.0	1.5	−1.6
	65	−0.7	1.2	−1.2	−1.0	2.0	−2.3
	75	−0.8	1.4	−1.7	−1.0	2.9	−3.0
	85	−0.8	2.1	−2.5	−1.1	2.7	−2.2
	Mean	−0.66	0.82	−0.86	−1.03	1.40	−1.45

temperature changes are larger at the midtroposphere than at the earth's surface for low and middle latitudes. This is in agreement with the results of model A.

The responses of the sensible and latent heat fluxes at the earth's surface to variations in solar constant for both models are shown in Table 4. As can be seen, the responses are quite different. The results of model A are in qualitative agreement with those of WM. Both model A and the GCM of WM show that as the solar constant increases the latent heat flux increases but the sensible heat flux decreases. As pointed out by Wetherald and Manabe, the nonlinear increase in saturation vapor pressure makes more energy available for evaporation and less energy available for sensible heat flux as the surface temperature increases. Contrary to the results of model A and WM, the changes in sensible and latent heat in model B are essentially in the same direction due to the linear relationship between them.

These results on sensitivity may be interpreted as follows. An increase of the solar constant makes more energy available for heating the earth's surface. With the nonlinear evaporation formulation, more of this energy is transferred to the atmosphere in the form of latent heat than with the linear evaporation formulation. As a result, in the nonlinear evaporation case, the temperature lapse rate tends to decrease; this induced a decrease in the sensible heat flux. The reverse is true for the linear evaporation case. That a smaller temperature lapse rate is associated with a decreased sensitivity of surface temperature to solar constant variations may be visualized through the following reasoning. Schneider and Mass (1975) show that the sensitivity of surface temperature to solar constant variations is inversely dependent on dF/dT_s, the change of the outgoing longwave radiation flux F with a change in surface temperature. In general, we may assume that the outgoing longwave radiation is a function not only of surface temperature but also of the tempera-

TABLE 4. Percentage changes of sensible and latent heat fluxes at the earth's surface due to the variations in solar constant for models A and B (with ice feedback). SH, upward flux of sensible heat; LH, upward flux of latent heat; WM, general circulation model of Wetherald and Manabe (1975). Numbers in parentheses indicate the hemispheric mean values for the standard cases (W m^{-2}).

	Model A		Model B		WM		
Change of solar constant (%)	0 → +1	0 → −1	0 → +1	0 → −1	0 → +2	0 → −2	−2 → −4
SH	(26.4) −2.9%	+2.9%	(37.3) +1.1%	−1.0%	(27.2) −5.1%	+0%	+7.7%
LH	(83.3) +3.5%	−3.6%	(70.9) +2.1%	−2.3%	(75.3) +9.3%	−6.5%	−10.2%

ture lapse rate γ. Therefore, dF/dT_s may be expanded into

$$\frac{dF}{dT_s} = \left(\frac{\partial F}{\partial T_s}\right)_\gamma + \left(\frac{\partial F}{\partial \gamma}\right)_{T_s}\left(\frac{d\gamma}{dT_s}\right).$$

$(\partial F/\partial \gamma)_{T_s}$ is a negative quantity. That is, for a given surface temperature, the outgoing longwave radiation will decrease as the temperature lapse rate increases. Since the magnitudes of $(\partial F/\partial T_s)_\gamma$ in models A and B are about the same, the difference in dF/dT_s depends only on the difference in $d\gamma/dT_s$ between the two models. Since $d\gamma/dT_s$ is negative for model A and positive for model B, dF/dT_s is greater for the nonlinear evaporation formulation of model A, so that this model has a smaller sensitivity to changes in the solar constant.

4. Conclusion

Our study shows how different evaporation parameterizations can affect the sensitivity of a climate model to solar constant variations. While both of the tested evaporation parameterizations yield similar model climates for the present solar constant, the sensitivity of the model climates to perturbations of solar constant is quite different for the two parameterizations. Compared to the linear evaporation formulation (model B), the nonlinear evaporation formulation (model A) is more effective in removing heat from the surface to the atmosphere, and the surface temperature appears to be less sensitive to solar constant variations.

Acknowledgment. The work was performed while one of us (SHC) was with Computer Sciences Corporation under NASA Contract NAS5-24350.

REFERENCES

Budyko, M. I., 1963: *Atlas of the Heat Balance of the Earth*. Gidrometeorizdat, Moscow, 69 pp. [NTIS 78A46579].

——, 1974: *Climate and Life*. Academic Press, 508 pp.

Charney, J., W. J. Quirk, S. Chow and J. Kornfield, 1977: A comparative study of the effects of albedo change on drought in semi-arid regions. *J. Atmos. Sci.*, **34**, 1366–1385.

Curran, R. J., R. Wexler and M. L. Nack. 1978: Albedo climatology analyses and the determination of fractional cloud cover. NASA Tech. Memo. 79576, 45 pp. [Available from Climate and Radiations Branch, Laboratory for Atmospheric Sciences, NASA/Goddard Space Flight Center, Greenbelt, MD 20771].

Lacis, A. A., and J. E. Hansen, 1974: A parameterization for the absorption of solar radiation in the earth's atmosphere. *J. Atmos. Sci.*, **31**, 113–133.

London, J., 1957: A study of the atmospheric heat balance. Final Report, Contract AF 19 (122)-165, College of Engineering, Dept. of Meteorology and Oceanography, New York University, 99 pp. [NTIS No. PB115626].

Manabe, S., 1969: Climate and the ocean circulation. 1. The atmospheric circulation and the hydrology of the earth's surface. *Mon. Wea. Rev.*, **97**, 739–774.

Newell, R. E., J. W. Kidson, D. G. Vincent and G. J. Boer, 1972: *The General Circulation of the Tropical Atmosphere and Interactions with Extra-tropical Latitudes*. MIT Press, 258 pp.

Ohring, G., and S. Adler, 1978: Some experiments with a zonally averaged climate model. *J. Atmos. Sci.*, **35**, 186–205.

Oort, A. H., and E. M. Rasmusson, 1971: *Atmospheric Circulation Statistics*. NOAA Prof. Pap. 5, 323 pp. [NTIS No. 72N20553].

Posey, J. W., and P. F. Clapp, 1964: Global distribution of normal surface albedo. *Geofis. Int.*, **4**, 33–48.

Saltzman, B., 1967: On the theory of the mean temperature of the earth's surface. *Tellus*, **19**, 219–229.

——, 1968: Steady state solutions for axially-symmetric climatic variables. *Pure Appl. Geophys.*, **69**, 237–259.

——, and A. D. Vernekar, 1971: An equilibrium solution for the axially symmetric component of the earth's macroclimate. *J. Geophys. Res.*, **76**, 1498–1524.

——, and ——, 1972: Global equilibrium solutions for the zonally averaged macroclimate. *J. Geophys. Res.*, **77**, 3936–3945.

Schneider, S. H., and C. Mass, 1975: Volcanic dusts, sunspots and temperature trends. *Science*, **190**, 741–746.

Sela, J., and A. Wiin-Nielsen, 1971: Simulation of the atmospheric annual energy cycle. *Mon. Wea. Rev.*, **99**, 460–468.

Sellers, W. D., 1965: *Physical Climatology*. University of Chicago Press, 272 pp.

——, 1973: A new global climatic model. *J. Appl. Meteor.*, **12**, 241–254.

Stone, P. H., S. Chow and W. J. Quirk, 1977: The July climate and a comparison of the January and July climates simulated by the GISS general circulation mode. *Mon. Wea. Rev.*, **105**, 170–194.

Vernekar, A. D., and H. D. Chang, 1978: A statistical-dynamical model for stationary perturbations in the atmosphere. *J. Atmos. Sci.*, **35**, 433–444.

Wetherald, R. T., and S. Manabe, 1975: The effects of changing the solar constant on the climate of a general circulation mode. *J. Atmos. Sci.*, **32**, 2044–2059.

Wiin-Nielsen, A., and H. Fuenzalida, 1975: On the simulation of the axisymmetric circulation of the atmosphere. *Tellus*, **27**, 199–214.